AIP Advances

Improvement in soft magnetic properties of thin bilayer ribbons using magnetoelastic effect

Cite as: AIP Advances **13**, 015032 (2023); https://doi.org/10.1063/9.0000598
Submitted: 03 October 2022 • Accepted: 16 November 2022 • Published Online: 30 January 2023

Takeshi Yanai, Yuka Yamaguchi, Yuhi Hayashida, et al.

Improvement in soft magnetic properties of thin bilayer ribbons using magnetoelastic effect

Cite as: AIP Advances 13, 015032 (2023); doi: 10.1063/9.0000598
Submitted: 3 October 2022 • Accepted: 16 November 2022 •
Published Online: 30 January 2023

Takeshi Yanai, Yuka Yamaguchi,[a] Yuhi Hayashida, Akihiro Yamashita, Masaki Nakano, and Hirotoshi Fukunaga

AFFILIATIONS

Nagasaki University, 1-14 Bunkyo-machi, Nagasaki 852-8521, Japan

Note: This paper was presented at the 67th Annual Conference on Magnetism and Magnetic Materials.
[a]**Author to whom correspondence should be addressed:** bb52122242@ms.nagasaki-u.ac.jp

ABSTRACT

We have prepared Fe-Ni-system bilayer ribbons with different magnetostriction (compositions) and investigated the improvement of soft magnetic properties using the magnetoelastic effect. A toroidal core with $D = 10$ mm was made from the $Fe_6Ni_{94}/Fe_{56}Ni_{44}$ bilayer ribbon, and the B-H loop of the core was measured. The shape of the hysteresis loop dramatically changed depending on the inner layer (inner magnetic phase). This result indicates that the direction of the anisotropy induced by bending stress was changed depending on the inner layer. The slope of the B-H loop and coercivity reduced when the $Fe_{56}Ni_{44}$ layer was on the inner side. From the experimental results, we found that domain rotation was dominant for the magnetization process. Consequently, the increase in the coercivity over frequency could be suppressed by controlling the magnetization process. From these results, we found that a thin bilayer ribbon with positive and negative magnetostriction constant is an attractive material for reducing iron losses under high frequency.

I. INTRODUCTION

In recent years, power semiconductors such as SiC and GaN have been rapidly developed,[1] and electric power and driving frequency in power-electronics-related equipment have gradually increased. From the trend of increases in power and frequency, metallic soft magnetic materials for magnetic devices, which can be used at high frequency, have been strongly required. When driving metallic materials at a high frequency, we need to reduce the thickness of the materials or control the magnetization process (the direction of anisotropy) to reduce eddy current loss.[2–5] We, therefore, focused on the magnetoelastic effect to reduce iron loss (hysteresis and eddy current losses). In the present study, we employed an electroplating method to prepare thin bilayer ribbons and investigated the improvement in the magnetic properties at high frequencies using the magnetoelastic effect.

II. PRINCIPLE OF REDUCTION IN IRON LOSS

Soft magnetic ribbons are typically used within toroidal cores. When the ribbon forms into a toroidal shape, bending stress is introduced into the ribbon. The stresses of the outer side and the inner ones are tension and compression, respectively. Figure 1 shows a schematic representation of the induction of anisotropy using the magnetoelastic effect (inverse magnetoelastic effect) in a bilayer ribbon with positive and negative magnetostriction constants, λ_s. When λ_s of the inner layer is positive, the direction of the induced anisotropy by the compressive stress is perpendicular to the ribbon axis. As the anisotropy direction for the outside layer ($\lambda_s < 0$) is also perpendicular, we can obtain the ribbon with uniaxial anisotropy by using the bending stress. In the case of Fig. 1, since the hard axis of magnetization is in the excitation direction, the domain rotation becomes dominant in the magnetization process of the ribbon and the hysteresis loss becomes theoretically zero. Under the same excitation conditions, as the eddy current for the domain rotation is generally smaller than that for the domain wall displacement the low iron loss (hysteresis and eddy current losses) is realized by the control of the anisotropy direction.

As shown in Fig. 1, we need positive and negative magnetostriction constants in each layer to obtain uniaxial anisotropy. It is well-known that the magnetostriction constant of Fe-Ni alloys depends on the composition,[6] indicating that the Fe-Ni alloy is a prefer-

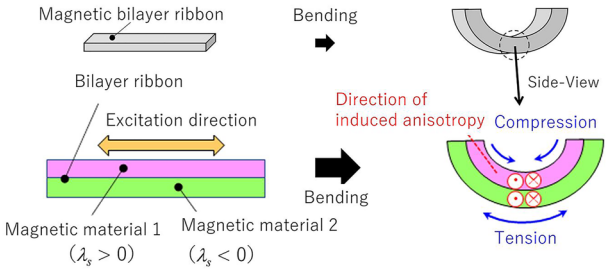

FIG. 1. Schematic representation (side-view) of induction of anisotropy in a bilayer ribbon using magnetoelastic effect.

able material for theoretical verification of Fig. 1. We, therefore, employed Fe-Ni system bilayer ribbons in this experiment.

III. EXPERIMENTAL PROCEDURES

A. Preparation of bilayer Fe-Ni ribbons

Some magnetic bilayer ribbons using melt-spinning methods with double nozzles were reported.[7–9] Although the multi-nozzle method is an attractive technique for the mass production of multilayered ribbons, thin ribbons (<10 μm) cannot be obtained. We, therefore, focused on another fabrication process of electroplating to obtain soft magnetic bilayer thin ribbons. Figure 2 shows the schematic representation of the electroplating. Tables I and II show the bath and electroplating conditions, respectively. The conditions were determined based on our previous studies.[10,11]

To construct a bilayer structure, we prepared two plating baths with different amounts of Fe reagent. Firstly, we electroplated

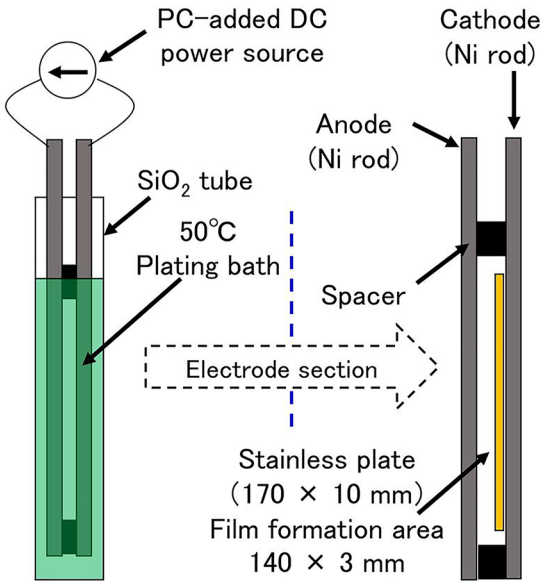

FIG. 2. Schematic representation of a fabrication process of a long Fe-Ni ribbon using an electroplating method.

TABLE I. Plating bath conditions.

Reagent	Concentration (g/l)
$NiCl_2{\cdot}6H_2O$ (Nickel chloride)	200, 275
$FeCl_2{\cdot}4H_2O$ (iron chloride)	5–70
$C_3H_4(OH)(COOH)_3{\cdot}H_2O$ (Citric acid)	5
$Na_3C_6H_5O_7{\cdot}2H_2O$ (tri-sodium citrate)	5
NaCl	5
$C_7H_4NNaO_3{\cdot}2H_2O$ (saccharin)	5

TABLE II. Plating conditions.

Conditions	Values
Anode/substrate	Ni/stainless
Bath temperature	50 °C
Current density	0.2 A/cm^2
Plating time	30–180 sec

Fe-poor (<10 at. %-Fe, $\lambda_s < 0$) films on a stainless substrate and then electroplated Fe-rich (>30 at. %-Fe, $\lambda_s > 0$) films on the Fe-poor ones. The film composition was controlled by changing the amount of the Fe reagent. After the electroplating, we peeled the bilayer film off the substrate and obtained 140 mm-long ribbons.

B. Annealing

As-peeled ribbons were sometimes curled depending on the plating conditions, as shown in Fig. 3(a). To obtain straight ribbons, we employed a joule-annealing method. The ribbons were joule-annealed under tensile stress ($j \approx 70$ A/mm^2, $\sigma \approx 50$ MPa, $t \approx 200$ sec) to remove the residual stress in the as-peeled ribbons, as shown in Fig. 3(b).

C. Evaluations

The thickness and the composition of the Fe-Ni ribbon were measured with a micrometer (Mitutoyo, CPM15-25MJ) and SEM-EDX (Hitachi High Technology, S-300), respectively. Dc-hysteresis loops of the straight-shaped ribbons were evaluated with a B-H curve tracer (RIKEN DENSHI, BHS-40), and we obtained the coercivity from the measured loop. To apply the bending stress to the ribbon, the ribbon formed into a toroidal core using a 3D-printed bobbin shown in Fig. 4, and the ac magnetic properties of the

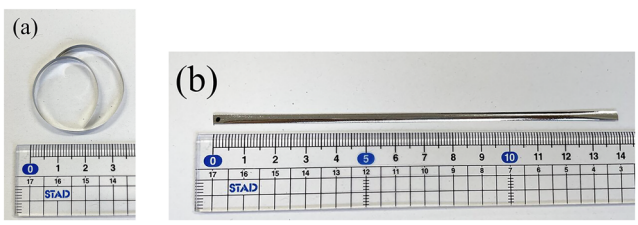

FIG. 3. Photographs of the long Fe-Ni bilayer ribbons before and after the joule-annealing. (a) As-peeled ribbon (b) Joule-annealed ribbon.

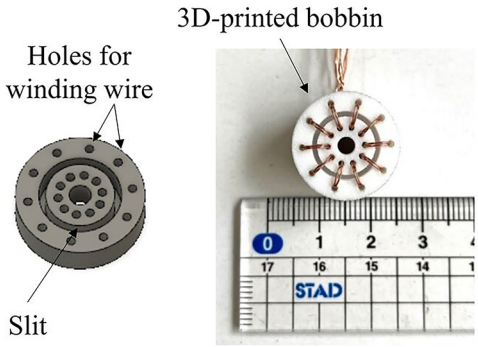

FIG. 4. 3D-model and photograph of the core bobbin for measurement of ac magnetic properties.

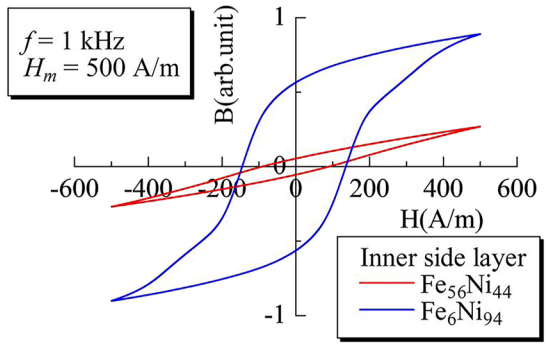

FIG. 6. B-H loops of a toroidal core made from the $Fe_6Ni_{94}/Fe_{56}Ni_{44}$ bilayer ribbon.

core were evaluated with a B-H analyzer (IWATSU, SY-8218). The diameter of the core is 10 mm, and we inserted the ribbon into the slit of the bobbin. To obtain the same winding condition for every evaluation, the winding wire passed through the holes in the bobbin.

IV. EXPERIMENTAL RESULTS AND DISCUSSION

Firstly, we evaluated the dc magnetic properties of the single-layered Fe-Ni ribbons. Figure 5 shows the coercivity as a function of the amount of the Fe reagent. In this experiment, the amount of the Ni reagent was fixed at 275 g/l. As shown in Fig. 5, low coercivity could be obtained at around 40 g/l of the Fe reagent. From the evaluation of the film composition, the Fe content of the films prepared at 40 g/l was ~22 at. %. $Fe_{22}Ni_{78}$ is a well-known composition where both the magnetocrystalline anisotropy and the magnetostriction constants become nearly zero, and our films also showed low coercivity around $Fe_{22}Ni_{78}$. This result implies that the sign of the magnetostriction constant in the Fe-Ni alloys changes from negative to positive around the Fe content of ~22 at. %. Based on this result, we prepared Fe-poor films (<10 at. %-Fe) as a negative magnetostriction phase and Fe-rich films (>30 at. %-Fe) as a positive magnetostriction one.

Figure 6 shows the hysteresis loops of the cores made from the $Fe_6Ni_{94}/Fe_{56}Ni_{44}$ bilayer ribbon. The difference between the two loops can be found in the inner side layer at the toroidal formation of the ribbon. The same bilayer ribbon was used for the toroidal formation, and the blue and red loops are for the inner layer of Fe_6Ni_{94} and $Fe_{56}Ni_{44}$, respectively. An obvious difference was observed between the two loops. As mentioned above, the signs of magnetostriction constant for the Fe-poor phase (Fe_6Ni_{94}) and Fe-rich one ($Fe_{56}Ni_{44}$) are negative and positive, respectively. In the case of the inner layer of $Fe_{56}Ni_{44}$, the directions of the induced anisotropy by the bending stress are perpendicular to the ribbon axis as shown in Fig. 1, indicating that the easy axis of magnetization is formed perpendicular to the ribbon axis. Consequently, the slope of the B-H loop and the hysteresis loss decrease. Both the slope and coercivity of the red loop decreased compared with those for the blue one, and we confirmed that the expected anisotropy as shown in Fig. 1 was induced.

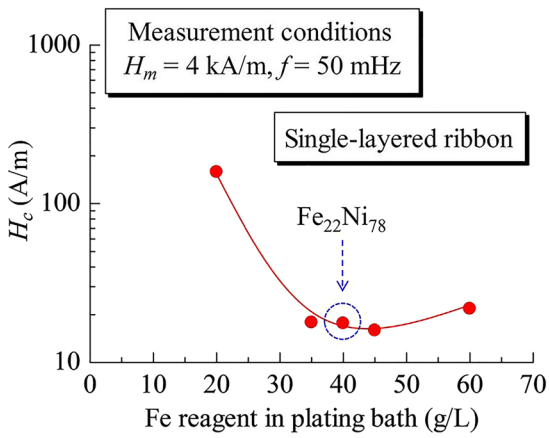

FIG. 5. Coercivity of the single-layered Fe-Ni ribbons as a function of the amount of the Fe reagent in the plating baths.

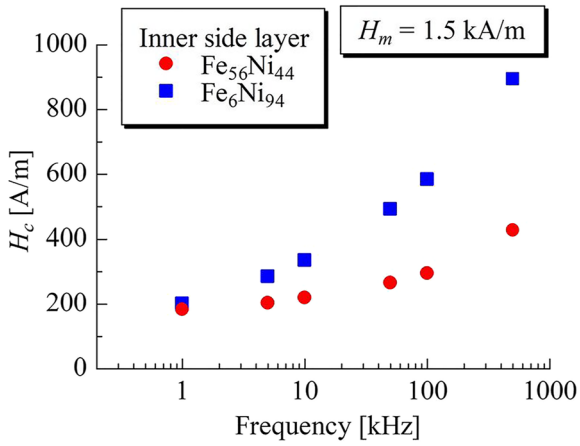

FIG. 7. Coercivity of the toroidal core prepared from the $Fe_6Ni_{94}/Fe_{56}Ni_{44}$ bilayer ribbon as a function of frequency.

Figure 7 shows the coercivity of the cores made from the $Fe_6Ni_{94}/Fe_{56}Ni_{44}$ bilayer ribbon as a function of exciting frequency. The symbols of "■" and "•" in Fig. 7 are the results for the inner layer of Fe_6Ni_{94} and $Fe_{56}Ni_{44}$, respectively. As shown in Fig. 7, the coercivity for "•" was smaller than that for "■" in all frequencies. In particular, we observed a large difference in H_c at a high frequency due to different magnetization processes: domain wall motion is for "■" and domain rotation is for "•". In the case of "•", as magnetized by domain rotation, we considered that an increase in the coercivity could be suppressed.

From these results, we found that thin bilayer ribbons with positive and negative magnetostriction are an attractive structure for high-frequency applications.

V. CONCLUSION

We investigated the improvement in the soft magnetic properties of thin bilayer ribbons focusing on the magnetoelastic effect. The obtained results are summarized as follows:

(1) The shape of the hysteresis loops of the toroidal core was changed dramatically corresponding to the inner layer.
(2) The slope of the B-H loop and the coercivity were decreased when the Fe-rich phase ($Fe_{56}Ni_{44}$) was selected as the inner layer. In such a case, the anisotropy is induced perpendicular to the ribbon axis, and the ribbon is magnetized by domain rotation.
(3) In the evaluation of the frequency dependence of the coercivity, the core with perpendicular anisotropy showed low coercivity.

AUTHOR DECLARATIONS

Conflict of Interest

The authors have no conflicts to disclose.

Author Contributions

Takeshi Yanai: Writing – original draft (equal). **Yuka Yamaguchi**: Writing – original draft (equal). **Yuhi Hayashida**: Writing – original draft (equal). **Akihiro Yamashita**: Writing – original draft (equal). **Masaki Nakano**: Writing – original draft (equal). **Hirotoshi Fukunaga**: Writing – original draft (equal).

DATA AVAILABILITY

The data that support the findings of this study are available from the corresponding author upon reasonable request.

REFERENCES

[1] F. Roccaforte, P. Fiorenza, G. Greco, R. Lo Nigro, F. Giannazzo, F. Iucolano, and M. Saggio, "Emerging trends in wide band gap semiconductors (SiC and GaN) technology for power devices," Microelectronic Engineering **187–188**, 66–77 (2018).
[2] Z. Li, K. Yao, D. Li, X. Ni, and Z. Lu, "Core loss analysis of Finemet type nanocrystalline alloy ribbon with different thickness," Progress in Natural Science: Materials International **27**, 588–592 (2017).
[3] A. Masood, H. A. Baghbaderani, K. L. Alvarez, J. M. Blanco, Z. Pavlovic, V. Ström, P. Stamenov, C. O. Mathuna, and P. McCloskey, "High-frequency power loss mechanisms in ultra-thin amorphous ribbons," Journal of Magnetism and Magnetic Materials **519**, 167469 (2021).
[4] Y. Yoshizawa and K. Yamauchi, "Effects of magnetic field annealing on magnetic properties in ultrafine crystalline Fe-Cu-Nb-Si-B alloys," IEEE Transactions on Magnetics **25**, 3324–3326 (1989).
[5] F. Fiorillo, E. Ferrara, M. Coïsson, C. Beatrice, and N. Banu, "Magnetic properties of soft ferrites and amorphous ribbons up to radiofrequencies," Journal of Magnetism and Magnetic Material **322**, 1497–1504 (2010).
[6] R. M. Bozorth, *Ferromagnetism* (Wiley-IEEE Press, 1993), p. 31.
[7] A. Masood, H. A. Baghbaderani, V. Ström, P. Stamenov, P. McCloskey, C. Ó. Mathúna, and S. Kulkarni, "Fabrication and soft magnetic properties of rapidly quenched Co-Fe-B-Si-Nb ultra-thin amorphous ribbons," Journal of Magnetism and Magnetic Materials **483**, 54–58 (2019).
[8] A. K. Panda, S. Dey, R. K. Roy, S. Singh, and A. Mitra, "Influence of phase transformation on interfacial activity and bend sensitivity of rapidly quenched $Fe_{77.5}Si_{7.5}B_{15}/Co_{72.5}Si_{12.5}B_{15}$ bilayered magnetostrictive ribbons," Journal of Magnetism and Magnetic Materials **378**, 440–446 (2015).
[9] I. Giouroudi, J. Kosel, H. Pfützner, and W. Brenner, "Magnetostrictive bilayer sensor system for testing of rotating microdevices," Sensors and Actuators A: Physical **142**, 474–478 (2008).
[10] T. Shimokawa, T. Yanai, K. Takahashi, M. Nakano, K. Suzuki, and H. Fukunaga, "Soft magnetic properties of electrodeposited Fe-Ni films prepared in citric acid based bath," IEEE Transactions on Magnetics **48**, 2907–2909 (2012).
[11] T. Yanai, T. Shimokawa, Y. Watanabe, T. Ohgai, M. Nakano, K. Suzuki, and H. Fukunaga, "Effect of current density on magnetic properties of electrodeposited Fe-Ni films prepared in a citric-acid-based-bath," Journal of Applied Physics **115**, 17A325 (2014).